Molecular Biology of the Cell
Vol. 20, 4630–4639, November 15, 2009

Membrane Insertion of the Pleckstrin Homology Domain Variable Loop 1 Is Critical for Dynamin-catalyzed Vesicle Scission

Rajesh Ramachandran,*† Thomas J. Pucadyil,* Ya-Wen Liu, Sharmistha Acharya, Marilyn Leonard, Vasyl Lukiyanchuk, and Sandra L. Schmid

Department of Cell Biology, The Scripps Research Institute, La Jolla, CA 92037

Submitted August 13, 2009; Revised September 14, 2009; Accepted September 16, 2009
Monitoring Editor: David G. Drubin

The GTPase dynamin catalyzes the scission of deeply invaginated clathrin-coated pits at the plasma membrane, but the mechanisms governing dynamin-mediated membrane fission remain poorly understood. Through mutagenesis, we have altered the hydrophobic nature of the membrane-inserting variable loop 1 (VL1) of the pleckstrin homology (PH) domain of dynamin-1 and demonstrate that its stable insertion into the lipid bilayer is critical for high membrane curvature generation and subsequent membrane fission. Dynamin PH domain mutants defective in curvature generation regain function when assayed on precurved membrane templates in vitro, but they remain defective in the scission of clathrin-coated pits in vivo. These results demonstrate that, in concert with dynamin self-assembly, PH domain membrane insertion is essential for fission and vesicle release in vitro and for clathrin-mediated endocytosis in vivo.

INTRODUCTION

Generation of high membrane curvature at the neck of a deeply invaginated coated pit is a requisite for membrane fission and vesicle release in intracellular membrane-trafficking processes. Yet lipid bilayers resist bending. Induction of high membrane curvature therefore requires the action of specialized protein machineries that function either as direct or indirect effectors of membrane bending (McMahon and Gallop, 2005; Antonny, 2006; Zimmerberg and Kozlov, 2006; Campelo *et al.*, 2008). Protein coats such as COPI, COPII, and clathrin/adaptor complexes that transiently assemble on the cytosolic faces of cognate cellular membranes likely initiate the curvature generation required for membrane budding (McMahon and Mills, 2004). Yet growing evidence indicates that several non–coat-forming protein partners are required for greater membrane curvature generation at the emerging bud neck via direct interactions with the lipid bilayer (Lundmark *et al.*, 2008). Included in this class of proteins are the Arf family GTPases, Arf1 and Sar1, required for COPI- and COPII-coated vesicle budding, respectively (Lee *et al.*, 2005; Beck *et al.*, 2008; Krauss *et al.*, 2008).

Dynamin, a prototypical member of a large family of self-assembling GTPases involved in various intracellular membrane fission events, catalyzes the scission of deeply invaginated clathrin-coated pits (CCPs) from the plasma membrane (Hinshaw, 2000; Conner and Schmid, 2003; Praefcke and McMahon, 2004). However, its mechanism of action remains controversial. A direct mechanical role for dynamin-1 in membrane fission has been proposed based on its ability to deform and tubulate model liposomes in vitro via spontaneous self-assembly into helical supramolecular scaffolds (Hinshaw and Schmid, 1995; Sweitzer and Hinshaw, 1998). The global conformational changes that ensue upon GTP binding and cooperative GTP hydrolysis in these extended structures have been suggested to drive membrane fission and tube fragmentation (Stowell *et al.*, 1999; Zhang and Hinshaw, 2001; Chen *et al.*, 2004; Danino *et al.*, 2004; Roux *et al.*, 2006; Mears *et al.*, 2007). However, more recent studies suggest that dynamic, self-limited assemblies of dynamin generated in the presence of GTP impose regulated curvature scaffolds on the membrane to catalyze membrane fission by stochastic generation of a "hemifission" intermediate (Bashkirov *et al.*, 2008; Pucadyil and Schmid, 2008). Dynamin self-assembly and resultant membrane tube constriction are required in both models to mediate membrane fission.

Membrane curvature in vitro can be imposed either by interactions of a protein scaffold with the membrane (e.g., by coat or BAR domain-containing proteins), or generated by asymmetric protein insertion into the outer leaflet of a vesicle lipid bilayer (e.g., by Arf family GTPases or ENTH domain–containing proteins; McMahon and Gallop, 2005; Zimmerberg and Kozlov, 2006). Dynamin's ability to generate high curvature has predominantly been ascribed to its self-assembling scaffold activity. Indeed, dynamin mutants defective in self-assembly exhibit greatly reduced ability to tubulate and generate uniform high membrane curvature on liposomes (Song *et al.*, 2004; Ramachandran *et al.*, 2007). Dynamin has also been shown to be a membrane-active molecule capable of inserting a large surface area into phos-

This article was published online ahead of print in *MBC in Press* (http://www.molbiolcell.org/cgi/doi/10.1091/mbc.E09–08–0683) on September 25, 2009.

* These authors contributed equally to this work.

† Address as of May 2010: Department of Physiology and Biophysics, Case Western Reserve University School of Medicine, Cleveland, OH 44106 (rxr275@case.edu).

Address correspondence to: Sandra L. Schmid (slschmid@scripps.edu) or Rajesh Ramachandran (rajeshr@scripps.edu).

Abbreviations used: CCP, clathrin-coated pit; CCV, clathrin-coated vesicle; Dyn, dynamin; PH, pleckstrin homology; VL1, variable loop 1.

phoinositide-containing lipid monolayers (Burger *et al.*, 2000). Whether and to what degree this activity is required for curvature generation or for dynamin function in vivo remains unknown.

Dynamin interacts directly with the lipid bilayer via its PH domain and this interaction is thought to be mediated primarily through electrostatic interactions between a positively charged lipid-binding pocket and the negatively charged lipid headgroup of phosphatidylinositol-4,5-bisphosphate (PIP_2; Ferguson *et al.*, 1994; Zheng *et al.*, 1996). However, isolated dynamin PH domains bind membranes with very low affinity and require oligomerization for greatly enhanced membrane association (Klein *et al.*, 1998). We recently showed that the relatively hydrophobic variable loop 1 (VL1) of the dynamin-1 PH domain partially penetrates the outer leaflet of a PIP_2-containing lipid bilayer upon membrane association (Ramachandran and Schmid, 2008). However, a functional requirement for dynamin's membrane-insertion activity has not been established.

Here we demonstrate that membrane insertion of the dynamin PH domain VL1 is essential for efficient high membrane curvature generation, assembly-dependent GTPase activation, and membrane fission in vitro and for coated pit neck constriction and vesicle release in vivo.

MATERIALS AND METHODS

Transferrin Internalization Assay

tTA-HeLa cells expressing recombinant adenovirus encoding Dyn1 wild type (WT) or mutants were used to assess the internalization of biotinylated transferrin into avidin-inaccessible endocytic compartments as described previously (Damke *et al.*, 2001).

Preparation of Dynamin and Derivatives

cDNAs encoding human Dyn1 WT or mutants subcloned in pIEx-6 (Novagen, Madison, WI) were used for the transient transfection of Sf9 insect cells for protein expression according to the manufacturer's protocols. This system eliminates the need for virus production and yields of dynamin average ~2–5 mg/100 ml cells. RCLDyn1 and RCLDyn1 I533C were prepared as described previously (Ramachandran and Schmid, 2008). Dynamin was purified and stored according to our published protocols (Leonard *et al.*, 2005; Ramachandran *et al.*, 2007). The lone Cys thiol in RCLDyn1 I533C, RCLDyn1 G532C, and RCLDyn1 G532C/I533A was specifically labeled with the fluorophore NBD (IANBD amide; 7-nitrobenz-2-oxa-1,3-diazole; Invitrogen, Carlsbad, CA) according to procedures described previously (Ramachandran and Schmid, 2008). The efficiency of NBD labeling was determined to be ~60% for RCLDyn1 I533C and ~90% for both RCLDyn1 G532C and RCLDyn1 G532C/I533A using molar absorptivity coefficients of 25,000 M^{-1} cm^{-1} for NBD at 478 nm and 58,790 M^{-1} cm^{-1} for dynamin at 280 nm.

Preparation of Liposomes, Lipid Nanotubes, SUPER Templates, and Membrane Tethers

All phospholipids were purchased from Avanti Polar Lipids (Alabaster, AL). Liposomes of 0.1-μm diameter composed of 85 mol% 1,2-dioleoyl-*sn*-glycero-3-phosphocholine (DOPC) and 15 mol% porcine PIP_2 and preformed lipid nanotubes composed of 45 mol% DOPC, 15 mol% PIP_2, and 40 mol% C24:1 β-D-galactosyl ceramide (GalCer) were generated according to procedures described previously (Leonard *et al.*, 2005; Ramachandran *et al.*, 2007). Supported bilayers with excess membrane reservoir (SUPER) templates on 5-μm plain silica beads (Corpuscular, Cold Spring, NY) were prepared using liposomes composed of 79 mol% DOPC, 15 mol% DOPS, 5 mol% PIP_2, and 1 mol% of RhPE [1,2-dioleoyl-*sn*-glycero-3-phosphoethanolamine-*N*-(lissamine rhodamine B sulfonyl)] as described earlier (Pucadyil and Schmid, 2008). SUPER templates deposited on BSA-coated glass coverslips were rocked gently with 20-μm plain silica beads to draw out membrane tethers that were ~50–100 nm in diameter.

GTPase Assay

GTP was purchased from Jena Bioscience (Jena, Germany). Basal, lipid-stimulated, and lipid-independent, assembly-stimulated (in low salt) GTP hydrolysis rates of Dyn1 WT and its derivatives were monitored as a function of time using a malachite green–based colorimetric assay as described previously (Leonard *et al.*, 2005). GTP was used at a final concentration of 1 mM.

Sedimentation Assays for Membrane Binding and Membrane Fission

To determine membrane binding, dynamin was separated into liposome-bound (pellet, P) and soluble (supernatant, S) fractions by high-speed centrifugation as described earlier (Ramachandran *et al.*, 2007). The membrane fission efficiencies of dynamin and derivatives were determined using SUPER templates and low-speed centrifugation also as described earlier (Pucadyil and Schmid, 2008).

Fluorescence and Electron Microscopy

Fluorescence microscopy of RhPE-labeled SUPER templates, flow-generated membrane tubules (0.5–1.0-μm diameter), and membrane tethers (~50–100-nm diameter) pulled out from SUPER templates was performed exactly as described (Pucadyil and Schmid, 2008). Live cell epifluorescence imaging of retrovirus-infected Dyn2 knockout (KO) mouse fibroblasts (Liu *et al.*, 2008) expressing Tomato-clathrin light chain alongside C-terminal green fluorescent protein (GFP) fusion constructs of either Dyn1 WT or Dyn1 I533A was performed using an inverted Olympus IX-70 microscope (Melville, NY). Electron microscopy of adenovirus-infected tTA-HeLa cells overexpressing either Dyn1 WT or Dyn1 I533A or neither (uninfected control) was performed and coated-pit profiles were classified as described (Schmid and Carter, 1990). Given that vesicle uncoating is rapid upon internalization, coated vesicle structures closely apposed to the plasma membrane (i.e., within three clathrin-coated vesicle [CCV] diameters) were scored as deeply invaginated coated pits whose tethering narrow necks are not captured in these individual thin sections (class IV pits; see Figure 4B). This classification has been validated extensively in earlier studies under conditions where clathrin-mediated endocytosis (CME) is known to be inhibited (Sandvig *et al.*, 1987; Schmid and Carter, 1990; Damke *et al.*, 2001). Images were collected at a magnification of ×25,000. For electron microscopy (EM) of purified dynamin on preformed lipid nanotubes, 1.0 μM dynamin was mixed with 25 μM lipid in buffer containing 20 mM HEPES, pH 7.5, and 150 mM KCl and incubated at room temperature for 30 min. The mixture was then adsorbed onto carbon-coated grids and stained with 1% uranyl acetate. Images were collected as described previously at a magnification of ×180,000 (Ramachandran *et al.*, 2007).

RESULTS

I533, a Residue in VL1 of the PH Domain Is Essential for Dynamin-1 Function in Vivo

For site-specific fluorescence labeling of the dynamin-1 (Dyn1) PH domain, we had previously introduced a single reactive Cys residue within the VL1 loop by mutagenic substitution of an Ile at position 533 (I533C; Ramachandran and Schmid, 2008). This mutation was introduced in a Dyn1 derivative called RCLDyn1(reactive-Cys-less Dyn1), in which six of the seven native Cys were replaced with Ser, allowing for site-specific modification with the environmentally sensitive fluorophore, NBD. Fluorescently labeled RCLDyn1 I533C-NBD was indistinguishable from Dyn1 WT in all demonstrable in vitro activities, including basal and liposome-stimulated GTPase activities as well as target lipid-binding (Ramachandran and Schmid, 2008). However, when overexpressed in cells, unlabeled RCLDyn1 I533C was found to be a dominant-negative inhibitor of transferrin internalization (Figure 1A), suggesting either that one or more of the native cysteines and/or I533 are essential for dynamin function in vivo. We previously suggested the former possibility because I533 is not conserved between dynamin isoforms 1 and 2 and previous reports had indicated that the isoform specificity of I533 and the posttranslational S-nitrosylation of C607 play important roles for Dyn1 function in vivo (Artalejo *et al.*, 1997; Wang *et al.*, 2006).

Unexpectedly, we found that RCLDyn1 alone is not a dominant-negative inhibitor of clathrin-mediated endocytosis in vivo in tTA-HeLa cells (Figure 1A), suggesting that none of the native Cys-to-Ser substitutions are responsible for the inhibitory phenotype. These data instead suggested that the I533C mutation specifically impaired Dyn1 function in vivo, and indeed, introduction of this single-point mutation into WT dynamin (Dyn1 I533C) generated a dominant-negative mutant (Supplemental Figure S1).

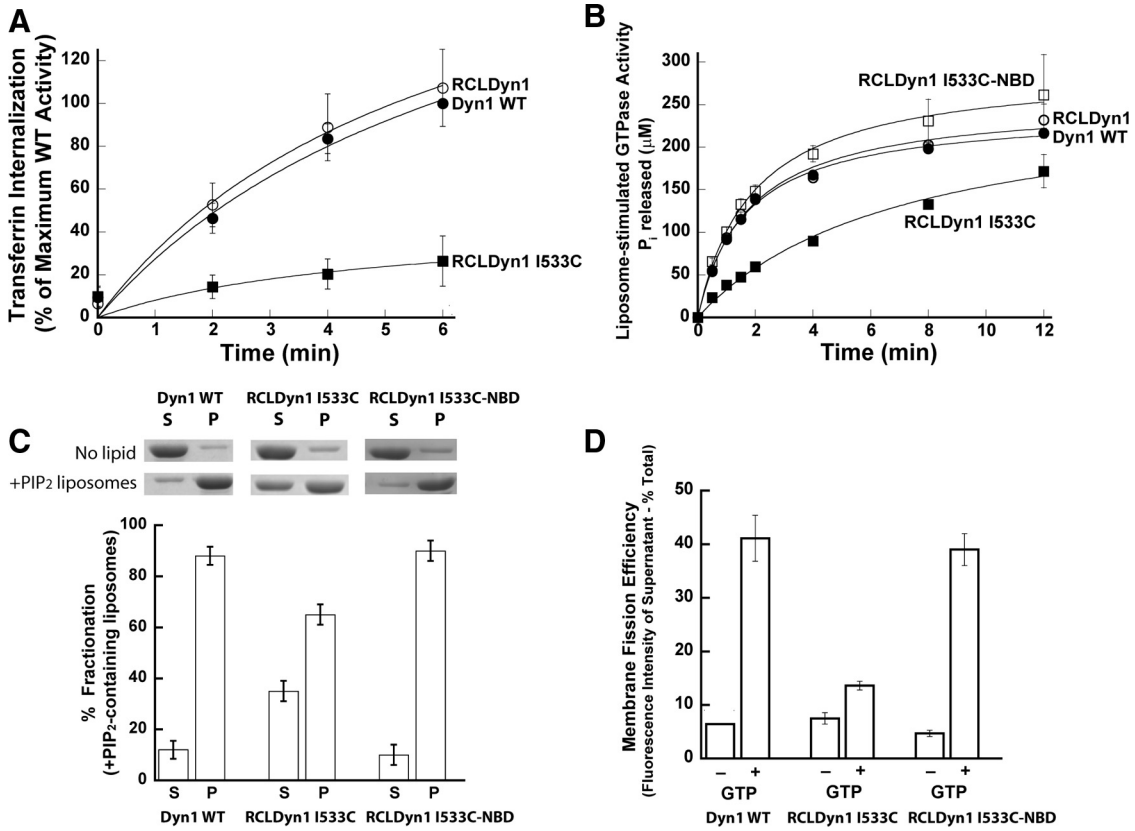

Figure 1. I533C mutation in VL1 impairs dynamin function in vivo and in vitro. (A) Transferrin uptake was followed in tTA-HeLa cells infected for 16–18 h with recombinant adenovirus encoding Dyn1 WT (●), RCLDyn1 (○), or RCLDyn1 I533C (■). The kinetics of internalization is plotted as a percentage of maximum uptake by Dyn1 WT. (B) Lipid-stimulated GTPase activities for 0.5 μM Dyn1 WT (●), RCLDyn1 (○), RCLDyn1 I533C (■), or RCLDyn1 I533C-NBD (□) preincubated with PIP_2-containing liposomes (150 μM total lipid) were measured at 37°C. The concentration of P_i released is plotted as a function of time. (C) Binding of 1.0 μM Dyn1 WT, RCLDyn1 I533C, or RCLDyn1 I533C-NBD to PIP_2-containing liposomes (300 μM lipid) was examined by sedimentation followed by SDS-PAGE analyses of supernatant (S) and pellet (P) fractions. Densitometric analyses of S and P fractions obtained using an Alpha Innotec Imager and FluorChem SP software (San Leandro, CA) are plotted. (D) Membrane fission activities of 0.5 μM Dyn 1 WT, unlabeled RCLDyn1 I533C, or fluorescently labeled RCLDyn1 I533C-NBD on RhPE-labeled SUPER templates (6 μM total lipid) in the constant presence of GTP (1 mM) were determined by a low-speed sedimentation assay as described in *Materials and Methods.* The fluorescence intensity of RhPE-labeled vesicles generated by membrane fission and recovered in the supernatant is plotted as a percentage of the total RhPE-labeled templates added to the assay. All values reported in this study represent the mean ± SD of at least three independent experiments.

Cys Mutation in VL1 Destabilizes Dynamin–Membrane Interactions

I533 is positioned at the base of the relatively hydrophobic VL1 in the PH domain (Ferguson *et al.*, 1994), which we previously showed inserts into the membrane (Ramachandran and Schmid, 2008). The substitution of either neighboring residues, Gly532 and Met534, individually with Cys (Dyn1 G532C or Dyn1 M534C) also resulted in a dominant-negative phenotype for transferrin internalization (Supplemental Figure S1), indicating the importance of the VL1 loop in dynamin function in vivo.

How can we reconcile the strong dominant-negative effect of RCLDyn1 I533C in vivo with the unperturbed activities of NBD-modified RCLDyn1 I533C in vitro? The experimentally determined hydrophobicities of Ile and Cys (with a protonated thiol) at the membrane–water interface are approximately equal (Wimley and White, 1996). Therefore, we reasoned that the partial negative charge on the Cys thiolate anion of RCLDyn1 I533C could electrostatically repel and thereby destabilize VL1 interactions with the negatively charged phosphatidylserine (PS)- and PIP_2-containing plasma membrane. Biochemical studies have previously shown that a Cys thiol located in a region of positive electrostatic potential, such as the lipid-binding pocket of the dynamin PH domain, tends to display an apparent pKa significantly lower than that observed for free Cys in solution (pKa ~8.3; Ferguson *et al.*, 1994; Liu *et al.*, 2004, 2006). Neutralization of this partial negative charge through covalent modification with a small, uncharged dye moiety such as NBD can therefore restore activity to WT levels (NBD properties reviewed in Heuck and Johnson, 2002; Johnson, 2005). Consistent with this interpretation, an uncharged Dyn1 G532S mutation, unlike Dyn1 G532C, is not a dominant-negative inhibitor of transferrin internalization (Vallis *et al.*, 1999).

To determine the nature of the biochemical defect responsible for the dominant-negative effect of the VL1 mutations, we characterized the biochemical properties of unlabeled RCLDyn1 I533C. This mutant exhibited partially reduced liposome-stimulated GTPase activity on PIP_2-containing liposomes compared with Dyn1 WT, RCLDyn1, and RCLDyn1 I533C-NBD (Figure 1B). Sedimentation analysis demonstrated that whereas nearly all of Dyn1 WT cosedimented with PIP_2-containing lipo-

somes, at equilibrium, only ~70% of RCLDyn1 I533C was found associated with membranes (Figure 1C), perhaps reflecting the fraction of Cys thiols in RCLDyn1 I533C in the uncharged, protonated state. Both the basal GTPase activity, measured in the absence of liposomes at physiological (150 mM KCl) ionic strength and the cooperative, assembly-stimulated GTPase activities measured at low (no KCl) ionic strength were comparable to those of Dyn1 WT (Supplemental Figure S2), indicating that the biochemical defects in RCLDyn1 I533C likely reflect a specific effect on membrane interactions.

We next assessed the ability of RCLDyn1 I533C mutant dynamin to mediate vesicle release from PIP_2-containing lipid bilayers supported on silica beads (SUPER templates; Pucadyil and Schmid, 2008). In contrast to the relatively modest and specific effects on membrane binding and liposome-stimulated GTPase activity, unlabeled RCLDyn1 I533C, as opposed to RCLDyn1 I533C-NBD, was dramatically impaired in its ability to catalyze membrane fission (Figure 1D). The extent of this defect correlated well with the inability of RCLDyn1 I533C to mediate CCV release in vivo.

Taken together, these data indicate that hydrophobic interactions between I533 of the Dyn1 PH domain VL1 and the membrane bilayer are critical for dynamin function in vitro and in vivo.

Hydrophobic Character of VL1 Is Required for Dynamin Function In Vivo and In Vitro

To further explore the role of VL1 in membrane association, we replaced I533 in Dyn1 with residues of varying side-chain hydrophobicities, based on the experimentally determined Wimley and White hydrophobicity scale for proteins at membrane–water interfaces (Wimley and White, 1996). Dyn1 I533W was chosen because aromatic residues are most favored at membrane–water interfaces, the experimentally determined location of Dyn1 VL1 (Ramachandran and Schmid, 2008). Mutations I533L and I533A were chosen for their vastly different hydrophobicities and bulk and also because Leu constitutes the corresponding residue in Dyn2 (Artalejo *et al.*, 1997).

The bulky and hydrophobic substitutions, I533W and I533L, had no appreciable effect on either the in vivo or in vitro properties of dynamin (Figure 2, A and B). In contrast, the less bulky I533A substitution showed dramatic effects (Figure 2, A and B). Similar to results observed for RCLDyn1 I533C (Figure 1), cells expressing Dyn1 I533A exhibited a strong dominant-negative phenotype for transferrin internalization (Figure 2A). This phenotype coincided with a ~90% reduction in the rate of liposome-stimulated GTP hydrolysis as well as a ~50% inhibition in dynamin–membrane association when Dyn1 I533A was assayed on liposomes in vitro (Figure 2, B and C). Furthermore, Dyn1 I533A displayed a severe defect in membrane fission and vesicle release from SUPER templates (Figure 2D). To rule out the possibility that the defects in liposome-stimulated GTPase activity and in membrane fission were due to the lower levels of membrane associated Dyn1 I533A, we tested whether these activities could be enhanced at higher concentrations of the mutant protein, which would increase the amount of membrane-associated dynamin by mass action. However, even at protein concentrations four times higher than WT, Dyn1 I533A remained defective in both liposome-stimulated GTPase activity and membrane fission (Supplemental Figure S3). These data indicate that membrane binding, assembly-dependent GTPase activation and membrane fission of Dyn1 are dependent on interactions between bulky, hydrophobic residues of VL1, namely I533 and M534, and the membrane bilayer.

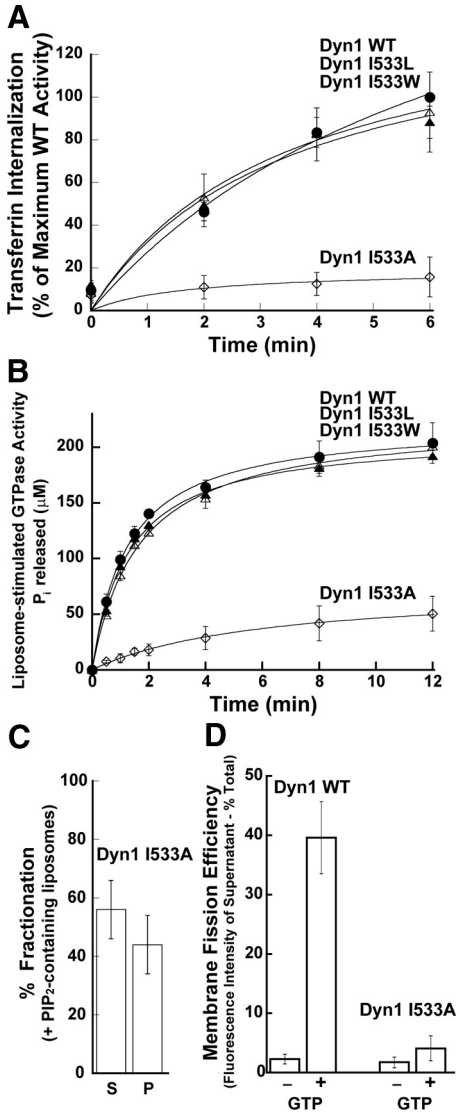

Figure 2. Hydrophobic VL1-membrane interactions are critical for dynamin function. (A) Kinetics of transferrin uptake in cells expressing Dyn1 WT (●), Dyn1 I533W (▲), Dyn1 I533L (△), or Dyn1 I533A (◇) were determined and plotted as in Figure 1A. (B) Lipid-stimulated GTPase activities of 0.5 μM Dyn1 WT (●), Dyn1 I533W (▲), Dyn1 I533L (△), or Dyn1 I533A (◇) preincubated with PIP_2-containing liposomes (150 μM total lipid) were obtained and plotted as in Figure 1B. (C) Sedimentation analysis of 1.0 μM Dyn1 I533A on PIP_2-containing liposomes (150 μM total lipid) was performed and plotted as in Figure 1C. (D) Membrane fission activities of 0.5 μM Dyn1 WT and Dyn1 I533A was determined on SUPER templates (6 μM total lipid) in the constant presence of GTP (1 mM) by a low-speed sedimentation assay as in Figure 1D.

VL1 Insertion Is Required for Efficient Membrane Curvature Generation

Our data suggest that interactions of the hydrophobic VL1 loop are important for stabilizing dynamin interactions on the membrane. We also previously showed using fluorescence quenching experiments that the VL1 loop inserts partially into the lipid bilayer (Ramachandran and Schmid,

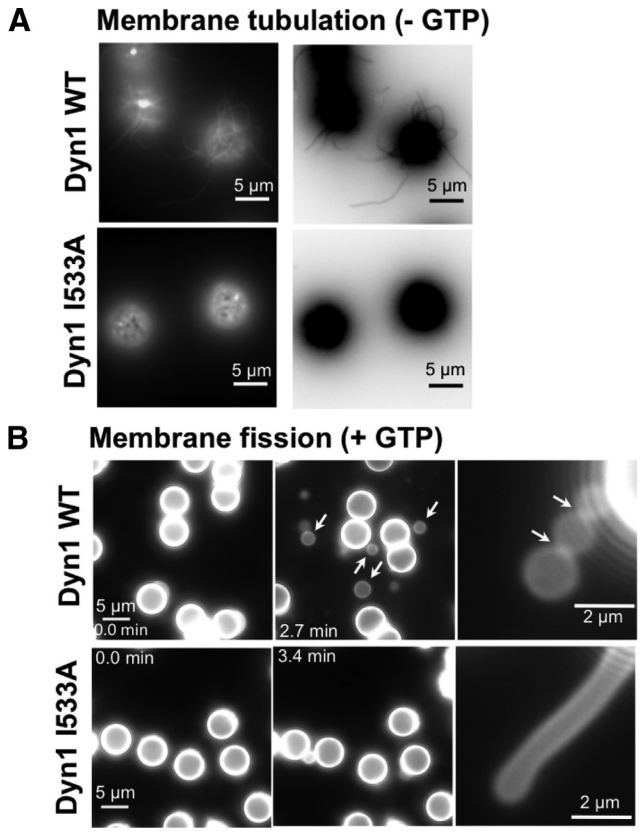

Figure 3. I533A VL1 mutant is defective in membrane curvature generation and membrane fission. (A) Fluorescence images of RhPE-labeled SUPER templates showing the effect of addition of either 0.5 μM Dyn1 WT or Dyn1 I533A in the absence of GTP. Images were acquired at a focal plane close to the coverslip. Contrast inverted images are also shown (right panels) for clarity. Note the absence of optically visible membrane tubules for Dyn1 I533A. (B) Fluorescence images showing the effect of addition of either 0.5 μM Dyn1 WT or Dyn1 I533A in the constant presence of GTP to membrane tubules (typically 0.5–1.0 μm in diameter) transiently generated by glycerol flow from RhPE-labeled SUPER templates (Pucadyil and Schmid, 2008). Left and middle, note the time-dependent release of vesicles (arrows) from the templates only in the case of Dyn1 WT. See Supplemental Movie 1 for entire sequence. Right, magnified fluorescence images showing visible membrane constrictions (arrows) before fission of flow-generated membrane tubules only in the case of Dyn1 WT.

2008). Together these properties suggest that VL1 may play a role in membrane curvature generation. We previously demonstrated that, in the absence of GTP, dynamin binds to and remodels planar lipid bilayers on SUPER templates to generate long membrane tubules that can be visualized by fluorescence microscopy (Pucadyil and Schmid, 2008). This assay provides a means to directly assess dynamin's curvature-generating activity. In contrast to Dyn1 WT, neither Dyn1 I533A (Figure 3A) nor Dyn1 I533C (Supplemental Figure S4A) could induce any optically visible membrane deformations, consistent with a defect in membrane curvature generation.

We next examined the ability of Dyn1 I533A to cooperatively assemble, constrict and catalyze fission of flow-generated membrane tubules formed from SUPER templates in the continuous presence of GTP as previously described (Pucadyil and Schmid, 2008). These flow-generated membrane tubules are typically 0.5–1.0 μm in diameter and can be considered planar in comparison to the much smaller dimensions of a soluble dynamin tetramer. Under these conditions, only Dyn1 WT generated the high membrane curvature required to form localized constrictions along the length of the emergent tubules (Figure 3B, top right panel, arrows and Supplemental Movie 1). These constricted tubules subsequently underwent membrane fission as detected by the release of large vesicles (Figure 3B, top middle panel, arrows). In contrast, we were unable to detect any membrane constrictions with either Dyn1 I533A (Figure 3B, bottom panel, and Supplemental Movie 1) or Dyn1 I533C (Supplemental Figure S4B). The inability of Dyn1 I533A to generate neck-like constrictions compared with Dyn1 WT strongly suggest that stable, hydrophobic interactions of the dynamin PH domain VL1 with the membrane bilayer are essential for efficient membrane curvature generation and membrane fission in vitro.

Dyn1 I533A Localizes to, But Fails to Constrict, Coated Pit Necks In Vivo

To determine whether the phenotype of Dyn1 I533A observed in vitro truly reflects its behavior in vivo, we first ascertained its localization at CCPs in living cells. Consistent with the role of SH3 domain-containing binding partners, and not the PH domain, in targeting dynamin to CCPs (Okamoto *et al.*, 1997; Bethoney *et al.*, 2009), the extent of colocalization of Dyn1 I533A with CCPs was similar to Dyn1 WT (Figure 4A). Next, we investigated the morphology of coated pits in cells overexpressing Dyn1 I533A in comparison to WT by EM, using previously established criteria to score accumulated CCP intermediates (see *Materials and Methods*). Consistent with a defect in high membrane curvature induction at the necks of invaginated CCPs required for membrane fission, Dyn1 I533A-expressing cells overwhelmingly accumulated deeply invaginated coated pits that remained tethered to the parent membrane. Cells expressing Dyn1 WT on the other hand exhibited a broad distribution of profiles comparable to control cells and consistent with continuous vesicle biogenesis and recycling (Figure 4B).

Collectively, the above data suggest that stable dynamin PH domain VL1 insertion into the membrane bilayer is essential for efficient membrane curvature generation at a membrane neck, and that this mechanical activity is absolutely necessary for dynamin-mediated membrane fission and vesicle release both in vitro and in vivo.

Precurved Lipid Nanotubes Rescue Membrane Curvature-defective Dynamin

Our data suggest that the primary defect of the Dyn1 I533A mutant is its reduced ability to efficiently generate membrane curvature, which is presumably dependent on stable insertion of the hydrophobic VL1 loop into the lipid bilayer. If so, the use of precurved membrane templates should rescue the phenotypic defects of Dyn1 I533A. True to our prediction, the steady state association of Dyn1 I533A with PIP_2-containing preformed lipid nanotubes, as measured by a sedimentation assay, was significantly higher than with liposomes, and indistinguishable from Dyn1 WT (Figure 5A, compare to Figure 2C). Furthermore, in contrast to the reduced GTPase activity observed on liposomes, Dyn1 I533A preincubated with lipid nanotubes exhibited nanotube-stimulated GTP hydrolysis rates similar to those of Dyn1 WT (Figure 5B). EM revealed that the helical packing of Dyn1 I533A on lipid nanotubes when incubated in the absence of GTP was also indistinguishable from that seen with Dyn1 WT (Figure 5C).

To more directly examine the effects of the I533A mutation on dynamin interactions with liposomes and lipid nano-

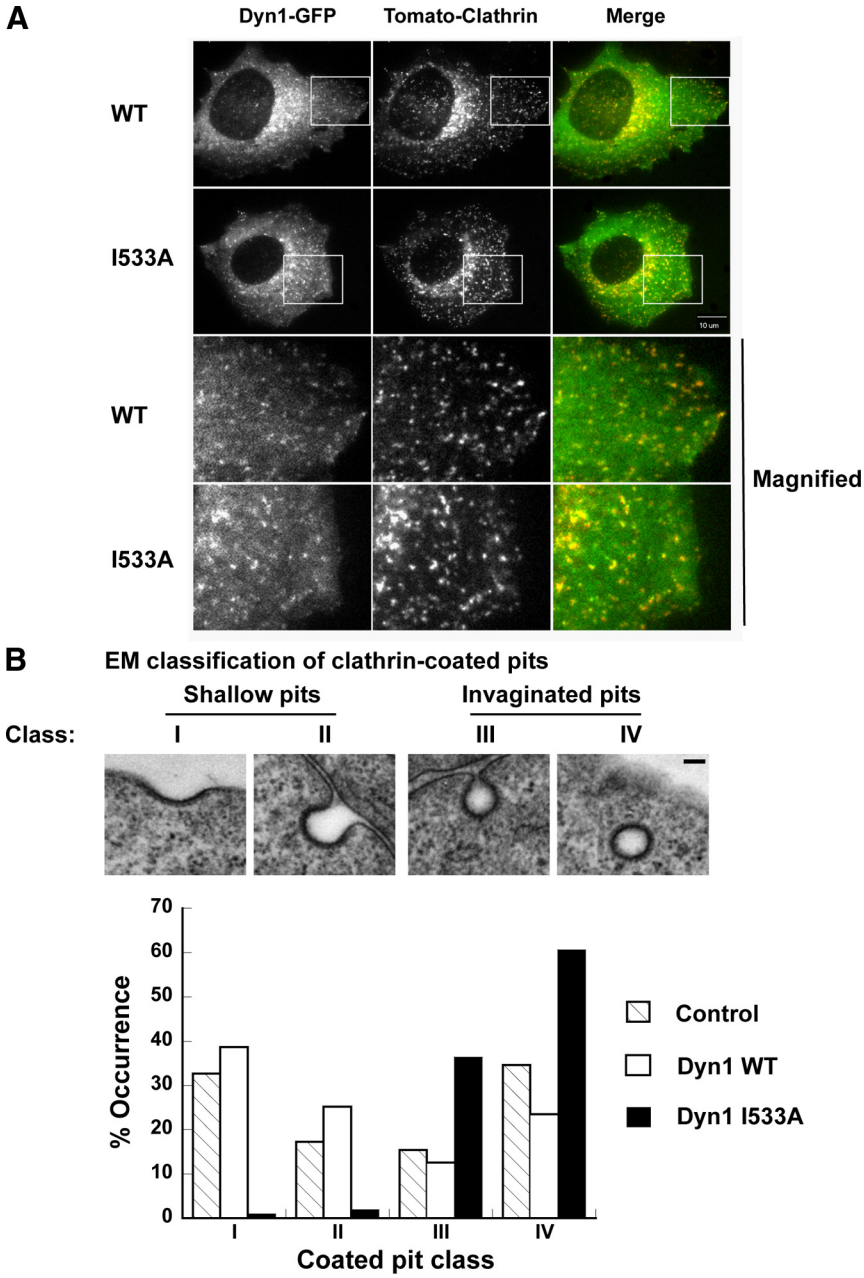

Figure 4. Dyn1 I533A targets to but fails to mediate fission of CCPs. (A) Top panels, live cell epifluorescence imaging of retrovirus-infected Dyn2 KO mouse fibroblasts expressing Tomato-clathrin light chain along with GFP fusion constructs of either Dyn1 WT or Dyn1 I533A. Scale bar, 10 μm. Bottom panels, magnified images from insets on top panels that demonstrate colocalization of clathrin and dynamin. (B) Top, EM classification of CCP profiles according to degree of membrane curvature and invagination. Classes I and II represent shallow, whereas classes III and IV represent deeply invaginated coated pits that remain tethered to the plasma membrane via a narrow membrane neck. Scale bar, 100 nm. Bottom, percent occurrence of these classes in tTA-HeLa cells overexpressing either Dyn1 WT (□) or Dyn1 I533A (■) or neither (▨) is plotted. Greater than 100 CCP profiles were scored for each sample.

tubes, we introduced a G532C mutation in VL1 of the PH domain of RCLDyn1 and RCLDyn1 I533A. This enabled site-specific covalent modification with the fluorescent dye NBD to yield RCLDyn1 G532C-NBD and RCLDyn1 G532C-NBD/I533A, respectively. The NBD-labeled derivatives demonstrated enzymatic (on liposomes) and membrane fission activities (on SUPER templates) comparable to those of Dyn1 WT and Dyn1 I533A, respectively (data not shown). Movement of the NBD dye from an aqueous to a nonpolar environment such as the hydrophobic core of a membrane bilayer is accompanied by a dramatic increase in its emission intensity, and this fluorescence change serves as a sensitive reporter of dynamin PH domain–membrane interactions (Ramachandran and Schmid, 2008).

Preincubation of RCLDyn1 G532C-NBD with liposomes in the absence of GTP resulted in an approximately eightfold increase in NBD intensity, as previously observed with RCLDyn1 I533C-NBD (Ramachandran and Schmid, 2008). As expected, given the ~50% reduced binding of Dyn1 I533A to liposomes, we observed only a approximately fourfold increase in NBD emission intensity for RCLDyn1 G532C-NBD/I533A (Figure 5D), ruling out artifacts due to dye labeling. In contrast to liposomes, after preincubation with lipid nanotubes, the NBD emission intensity increase for RCLDyn1 G532C-NBD/I533A was similar to that of RCLDyn1 G532C-NBD, indicating that nearly an equivalent fraction of Dyn1 I533A molecules associated with and was inserted into these precurved membrane templates (Figure 5D). These data are consistent with the nearly equivalent values for assembly-stimulated GTPase activity observed for Dyn1WT and Dyn1 I533A after preincubation with lipid nanotubes (Figure 5B) and demonstrate that the membrane binding and assembly-stimulated GTPase defects of the Dyn1 I533A mutant can be rescued when using a curved template.

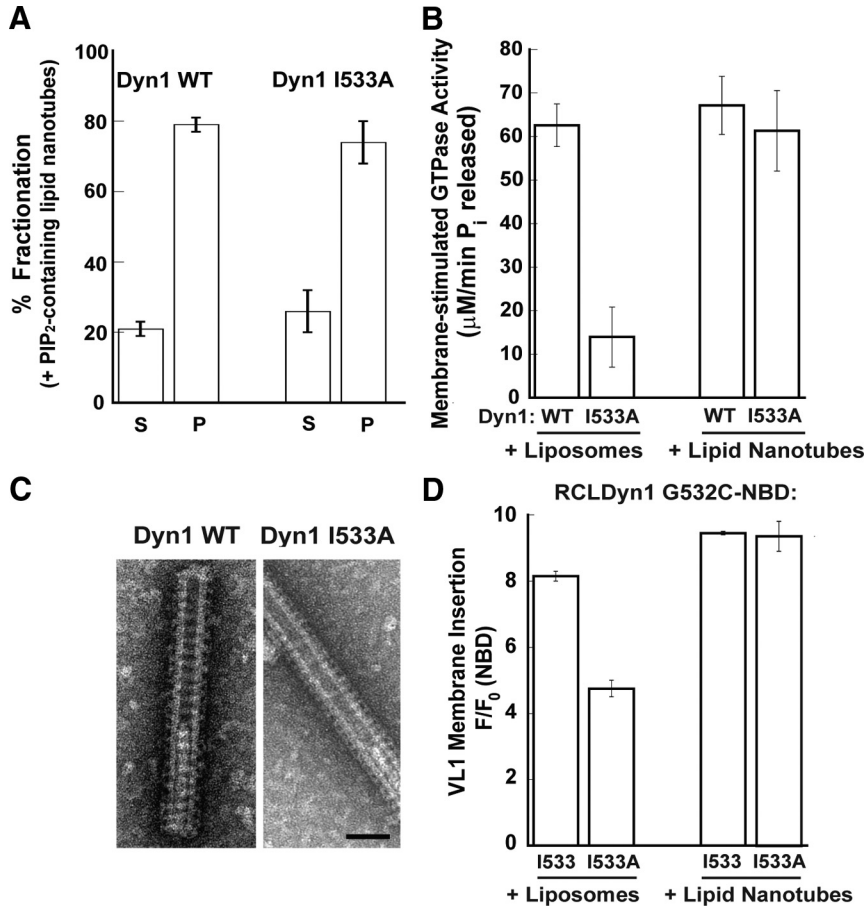

Figure 5. Precurved lipid templates rescue Dyn1 I533A. (A) Sedimentation analysis of 1.0 μM Dyn1 I533A on preformed PIP_2-containing lipid nanotubes (300 μM total lipid) was performed and plotted as in Figure 1C. (B) Assembly-stimulated GTP hydrolysis rate of 0.5 μM Dyn1 WT or Dyn1 I533A induced upon preincubation with either PIP_2-containing liposomes or PIP_2-containing lipid nanotubes (150 μM total lipid) is plotted as μM P_i released per minute. (C) Representative electron micrographs of Dyn1 WT and Dyn1 I533A self-assembled on PIP_2-containing lipid nanotubes. Scale bar, 50 nm. (D) The magnitude of VL1-membrane binding in 0.1 μM RCLDyn1 (G532C-NBD), I533 or I533A, was determined by detecting the fold increase in the steady-state emission intensity of NBD upon incubation with either PIP_2-containing liposomes or PIP_2-containing lipid nanotubes (30 μM total lipid). F/F_0 is the ratio of the emission intensity values obtained for NBD before (F_0) and after (F) incubation with the corresponding lipid templates.

Dyn1 I533A Can Mediate Fission of Precurved Membrane Tubes

That membrane association and resultant assembly-stimulated GTPase activity of Dyn1 I533A can be rescued on a curved membrane template provides strong evidence that membrane curvature generation is the primary defect of this mutant. Remarkably, the membrane fission activity of Dyn1 I533A can also be rescued. When incubated with membrane tubules pulled out from SUPER templates, the Dyn1 I533A mutant can catalyze its scission albeit with slower kinetics than WT (Figure 6 and Supplemental Movie 2). Similar results were obtained with Dyn1 I533C, which is also defective in membrane curvature induction (Supplemental Figure S4C). The enhanced ability of Dyn1 I533A to catalyze scission of precurved lipid membrane tubules (vs. relatively planar SUPER templates) correlated with a higher steady-

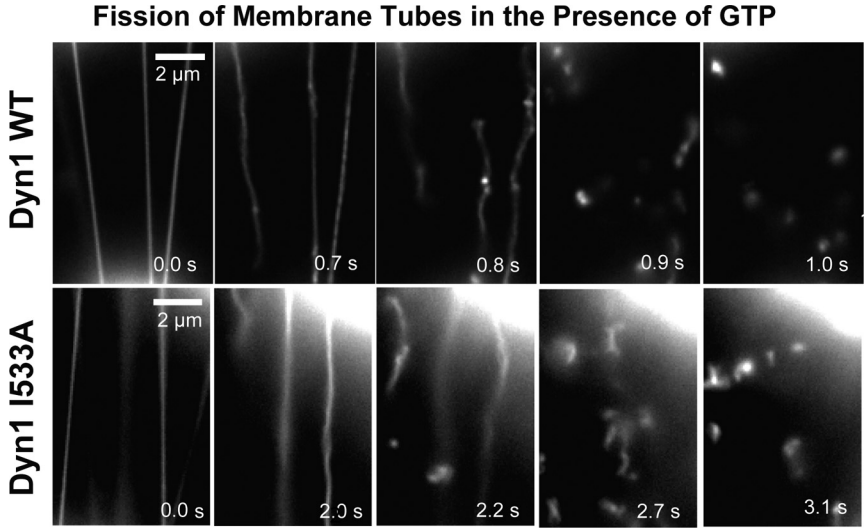

Figure 6. Fission of precurved membrane tubes mediated by Dyn1 I533A. Time-lapse fluorescence images showing the effect of addition of either 0.5 μM Dyn1 WT or Dyn1 I533A to membrane tethers (typically ~50–100-nm diameter) pulled out of RhPE-labeled SUPER templates in the presence of GTP (1 mM final). See Supplemental Movie 2 for entire sequence.

state association with precurved membranes (Figure 5, A and D). The ability of Dyn1 I533A and Dyn1 I533C to mediate fission of precurved templates in vitro despite a profound defect in mediating CME, suggests that dynamin functions to generate high membrane curvature at the necks of invaginated coated pits in vivo and facilitate membrane fission.

DISCUSSION

We have demonstrated that efficient membrane curvature generation by dynamin requires, in addition to its scaffolding properties, stable insertion of the relatively hydrophobic PH domain VL1 into the lipid bilayer and that this activity is critical for both membrane fission from SUPER templates in vitro and for dynamin function in endocytic CCV release in vivo.

Shallow membrane penetration utilizing a pair of adjacent, loop-residing hydrophobic residues (I533 and M534) is not unique to Dyn1 and has been demonstrated in various PH domains (Manna *et al.,* 2007). However, the dynamin PH domain is unlikely to be able to generate membrane curvature on its own. Previous studies have shown that the affinity of an isolated dynamin PH domain for the phosphoinositide headgroup is low, therefore necessitating dynamin oligomerization to sustain multivalent, high-avidity PH domain–membrane interactions (Klein *et al.,* 1998; Lemmon and Ferguson, 2000). Indeed, in our own studies with the isolated Dyn1 PH domain site-specifically labeled at position I533C with NBD (Dyn1 PH I533C-NBD), we were unable to detect any membrane binding or insertion (data not shown). We have previously shown that middle domain mutants, Dyn1 R399A and Dyn1 R361S, defective in dynamin self-assembly also exhibit a much reduced, albeit measurable, ability to generate membrane tubules from liposomes with correspondingly reduced liposome-stimulated GTPase activity (Ramachandran *et al.,* 2007). These mutants are unable to mediate either tubule formation or vesicle release from SUPER templates (Pucadyil & Schmid, 2008). Finally, like the VL1 mutants, assembly-defective Dyn1 mutants are also dominant-negative inhibitors of clathrin-mediated endocytosis in vivo (Song *et al.,* 2004). Together, these data demonstrate that both self-assembly and dynamin PH domain membrane insertion are *necessary* for the highly efficient membrane curvature induction required for dynamin function in vivo and that neither activity alone is *sufficient*.

We have argued that the dominant-negative phenotype caused by overexpression of the VL1 loop mutations (Dyn1 I533A or I533C) is due to their inability to efficiently generate high membrane curvature. However, in vitro analyses of the Dyn1 I533A and Dyn1 I533C mutant proteins revealed partial defects in liposome binding and liposome-stimulated GTPase activities. The following arguments support our belief that these defects per se do not account for the dominant-negative effects of these mutants on CCV release in vivo. First, the Dyn1 I533C mutation has only a mild defect in assembly-stimulated GTPase assay and liposome binding ($\leq$50% inhibited relative to WT) compared with the I533A mutation ($\sim$90% inhibited relative to WT), yet both had equally potent dominant-negative effects. Thus the degree of inhibition did not correlate with these in vitro phenotypes. Second, the in vitro membrane binding and assembly-stimulated GTPase defects could largely be rescued on precurved membrane templates, yet these mutants were unable to mediate CCV release in vivo. Thus, we conclude that the in vivo defect in Dyn1 I533A and Dyn1 I533C lies in their inability to efficiently induce high membrane curvature at the neck of a coated pit. We suggest that the I533A and I533C substitutions when compared with uncharged, bulky hydrophobic residues in I533W and I533L, create smaller "footprints" on the membrane surface and are therefore unable to force membrane curvature or stabilize dynamin-membrane association, both of which also require coincident dynamin self-assembly. In this regard it is important to note that, unlike Dyn1 I533A, the assembly-defective Dyn1 R399A mutant cannot be rescued on precurved lipid nanotubes for either self-assembly or assembly-stimulated GTPase activity (data not shown).

At what stage in CCV formation is dynamin-induced membrane curvature required? Although there is a burst of dynamin recruitment at late stages of CCV formation, it is also present, albeit at lower levels, on newly formed CCPs and an early role for dynamin at the nascent stages of coated pit formation has been well documented (Narayanan *et al.,* 2005; Macia *et al.,* 2006; Loerke *et al.,* 2009). Our observation that the I533A mutant can mediate fission given a sufficiently curved, preconstricted template in vitro, yet cannot support CCV formation in vivo, coupled with our finding that invaginated CCPs accumulate in cells expressing the dominant-negative Dyn1 I533A mutant, argues strongly that the in vivo defect must be immediately upstream of neck constriction. Here, by partially inserting into the lipid bilayer, self-assembled dynamin might function to generate further localized curvature to destabilize the membrane and facilitate fission and vesicle release. Curvature-generating molecules such as epsin, which are sufficient to generate budded CCPs from liposomes and planar lipid bilayers (Takei *et al.,* 1998; Ford *et al.,* 2002), together with BAR domain-containing dynamin binding partners, such as sorting nexin 9 and endophilin, could create the neck of the emerging bud and direct localized assembly and further curvature generation by dynamin. Thus, as suggested previously (Yoshida *et al.,* 2004; Ramachandran and Schmid, 2008), endocytic accessory factors are likely to function in concert with dynamin at the late stages of coated vesicle formation as curvature generators and/or stabilizers to enhance the potency of dynamin in membrane fission. Importantly, our findings establish that efficient curvature generation by dynamin insertion at the necks of deeply invaginated coated pits plays a critical role in membrane fission leading to endocytic CCV formation in vivo.

While this manuscript was under review, a recent article concluded that the dynamin PH domain might function to cluster PIP_2 at CCP necks to create a lipid gradient essential for fission (Bethoney *et al.,* 2009). Whereas we cannot rule out PH domain–mediated PIP_2 clustering during dynamin self-assembly as a passive contributor to membrane fission, our data instead demonstrate an active mechanical role for dynamin via VL1-membrane insertion in effecting vesicle scission. The recent observation that dynamin can catalyze nonleaky fission of membrane tubules lacking PIP_2 but containing PS (Bashkirov *et al.,* 2008) is also consistent with such a membrane-active mechanism for dynamin.

ACKNOWLEDGMENTS

We acknowledge Malcolm R. Wood for help with EM and thank colleagues in the Schmid lab for critical comments. This work is supported by grants from the National Institutes of Health to S.L.S. (R01.GM042455 and

R37.MH61345). R.R. is a special fellow and T.J.P. is a fellow of the Leukemia and Lymphoma society. Y-W.L. is supported by the Muscular Dystrophy Association. This is The Scripps Research Institute manuscript number TSRI-20071.

REFERENCES

Antonny, B. (2006). Membrane deformation by protein coats. Curr. Opin. Cell Biol. *18*, 386–394.

Artalejo, C. R., Lemmon, M. A., Schlessinger, J., and Palfrey, H. C. (1997). Specific role for the PH domain of dynamin-1 in the regulation of rapid endocytosis in adrenal chromaffin cells. EMBO J. *16*, 1565–1574.

Bashkirov, P. V., Akimov, S. A., Evseev, A. I., Schmid, S. L., Zimmerberg, J., and Frolov, V. A. (2008). GTPase cycle of dynamin is coupled to membrane squeeze and release, leading to spontaneous fission. Cell *135*, 1276–1286.

Beck, R., *et al*. (2008). Membrane curvature induced by Arf1-GTP is essential for vesicle formation. Proc. Natl. Acad. Sci. USA *105*, 11731–11736.

Bethoney, K. A., King, M. C., Hinshaw, J. E., Ostap, E. M., and Lemmon, M. A. (2009). A possible effector role for the pleckstrin homology (PH) domain of dynamin. Proc. Natl. Acad. Sci. USA *106*, 13359–13364.

Burger, K. N., Demel, R. A., Schmid, S. L., and de Kruijff, B. (2000). Dynamin is membrane-active: lipid insertion is induced by phosphoinositides and phosphatidic acid. Biochemistry *39*, 12485–12493.

Campelo, F., McMahon, H. T., and Kozlov, M. M. (2008). The hydrophobic insertion mechanism of membrane curvature generation by proteins. Biophys. J. *95*, 2325–2339.

Chen, Y. J., Zhang, P., Egelman, E. H., and Hinshaw, J. E. (2004). The stalk region of dynamin drives the constriction of dynamin tubes. Nat. Struct. Mol. Biol. *11*, 574–575.

Conner, S. D., and Schmid, S. L. (2003). Regulated portals of entry into the cell. Nature *422*, 37–44.

Damke, H., Binns, D. D., Ueda, H., Schmid, S. L., and Baba, T. (2001). Dynamin GTPase domain mutants block endocytic vesicle formation at morphologically distinct stages. Mol. Biol. Cell *12*, 2578–2589.

Danino, D., Moon, K. H., and Hinshaw, J. E. (2004). Rapid constriction of lipid bilayers by the mechanochemical enzyme dynamin. J. Struct. Biol. *147*, 259–267.

Ferguson, K. M., Lemmon, M. A., Schlessinger, J., and Sigler, P. B. (1994). Crystal structure at 2.2 A resolution of the pleckstrin homology domain from human dynamin. Cell *79*, 199–209.

Ford, M. G., Mills, I. G., Peter, B. J., Vallis, Y., Praefcke, G. J., Evans, P. R., and McMahon, H. T. (2002). Curvature of clathrin-coated pits driven by epsin. Nature *419*, 361–366.

Heuck, A. P., and Johnson, A. E. (2002). Pore-forming protein structure analysis in membranes using multiple independent fluorescence techniques. Cell Biochem. Biophys. *36*, 89–101.

Hinshaw, J. E. (2000). Dynamin and its role in membrane fission. Annu. Rev. Cell Dev. Biol. *16*, 483–519.

Hinshaw, J. E., and Schmid, S. L. (1995). Dynamin self-assembles into rings suggesting a mechanism for coated vesicle budding. Nature *374*, 190–192.

Johnson, A. E. (2005). Fluorescence approaches for determining protein conformations, interactions and mechanisms at membranes. Traffic *6*, 1078–1092.

Klein, D. E., Lee, A., Frank, D. W., Marks, M. S., and Lemmon, M. A. (1998). The pleckstrin homology domains of dynamin isoforms require oligomerization for high affinity phosphoinositide binding. J. Biol. Chem. *273*, 27725–27733.

Krauss, M., Jia, J. Y., Roux, A., Beck, R., Wieland, F. T., De Camilli, P., and Haucke, V. (2008). Arf1-GTP-induced tubule formation suggests a function of Arf family proteins in curvature acquisition at sites of vesicle budding. J. Biol. Chem. *283*, 27717–27723.

Lee, M. C., Orci, L., Hamamoto, S., Futai, E., Ravazzola, M., and Schekman, R. (2005). Sar1p N-terminal helix initiates membrane curvature and completes the fission of a COPII vesicle. Cell *122*, 605–617.

Lemmon, M. A., and Ferguson, K. M. (2000). Signal-dependent membrane targeting by pleckstrin homology (PH) domains. Biochem. J. *350*(Pt 1), 1–18.

Leonard, M., Song, B. D., Ramachandran, R., and Schmid, S. L. (2005). Robust colorimetric assays for dynamin's basal and stimulated GTPase activities. Methods Enzymol. *404*, 490–503.

Liu, X., Alexander, C., Serrano, J., Borg, E., and Dawson, D. C. (2006). Variable reactivity of an engineered cysteine at position 338 in cystic fibrosis transmembrane conductance regulator reflects different chemical states of the thiol. J. Biol. Chem. *281*, 8275–8285.

Liu, X., Zhang, Z. R., Fuller, M. D., Billingsley, J., McCarty, N. A., and Dawson, D. C. (2004). CFTR: a cysteine at position 338 in TM6 senses a positive electrostatic potential in the pore. Biophys. J. *87*, 3826–3841.

Liu, Y. W., Surka, M. C., Schroeter, T., Lukiyanchuk, V., and Schmid, S. L. (2008). Isoform and splice-variant specific functions of dynamin-2 revealed by analysis of conditional knock-out cells. Mol. Biol. Cell *19*, 5347–5359.

Loerke, D., Mettlen, M., Yarar, D., Jaqaman, K., Jaqaman, H., Danuser, G., and Schmid, S. L. (2009). Cargo and dynamin regulate clathrin-Coated pIt maturation. PLoS Biol. *7*, e57.

Lundmark, R., Doherty, G. J., Vallis, Y., Peter, B. J., and McMahon, H. T. (2008). Arf family GTP loading is activated by, and generates, positive membrane curvature. Biochem. J. *414*, 189–194.

Macia, E., Ehrlich, M., Massol, R., Boucrot, E., Brunner, C., and Kirchhausen, T. (2006). Dynasore, a cell-permeable inhibitor of dynamin. Dev. Cell *10*, 839–850.

Manna, D., Albanese, A., Park, W. S., and Cho, W. (2007). Mechanistic basis of differential cellular responses of phosphatidylinositol 3,4-bisphosphate- and phosphatidylinositol 3,4,5-trisphosphate-binding pleckstrin homology domains. J. Biol. Chem. *282*, 32093–32105.

McMahon, H. T., and Gallop, J. L. (2005). Membrane curvature and mechanisms of dynamic cell membrane remodelling. Nature *438*, 590–596.

McMahon, H. T., and Mills, I. G. (2004). COP and clathrin-coated vesicle budding: different pathways, common approaches. Curr. Opin. Cell Biol. *16*, 379–391.

Mears, J. A., Ray, P., and Hinshaw, J. E. (2007). A corkscrew model for dynamin constriction. Structure *15*, 1190–1202.

Narayanan, R., Leonard, M., Song, B. D., Schmid, S. L., and Ramaswami, M. (2005). An internal GAP domain negatively regulates presynaptic dynamin in vivo: a two-step model for dynamin function. J. Cell Biol. *169*, 117–126.

Okamoto, P. M., Herskovits, J. S., and Vallee, R. B. (1997). Role of the basic, proline-rich region of dynamin in Src homology 3 domain binding and endocytosis. J. Biol. Chem. *272*, 11629–11635.

Praefcke, G. J., and McMahon, H. T. (2004). The dynamin superfamily: universal membrane tubulation and fission molecules? Nat. Rev. Mol. Cell Biol. *5*, 133–147.

Pucadyil, T. J., and Schmid, S. L. (2008). Real-time visualization of dynamin-catalyzed membrane fission and vesicle release. Cell *135*, 1263–1275.

Ramachandran, R., and Schmid, S. L. (2008). Real-time detection reveals that effectors couple dynamin's GTP-dependent conformational changes to the membrane. EMBO J. *27*, 27–37.

Ramachandran, R., Surka, M., Chappie, J. S., Fowler, D. M., Foss, T. R., Song, B. D., and Schmid, S. L. (2007). The dynamin middle domain is critical for tetramerization and higher-order self-assembly. EMBO J. *26*, 559–566.

Roux, A., Uyhazi, K., Frost, A., and De Camilli, P. (2006). GTP-dependent twisting of dynamin implicates constriction and tension in membrane fission. Nature *441*, 528–531.

Sandvig, K., Olsnes, S., Petersen, O. W., and van Deurs, B. (1987). Acidification of the cytosol inhibits endocytosis from coated pits. J. Cell Biol. *105*, 679–689.

Schmid, S. L., and Carter, L. L. (1990). ATP is required for receptor-mediated endocytosis in intact cells. J. Cell Biol. *111*, 2307–2318.

Song, B. D., Yarar, D., and Schmid, S. L. (2004). An assembly-incompetent mutant establishes a requirement for dynamin self-assembly in clathrin-mediated endocytosis in vivo. Mol. Biol. Cell *15*, 2243–2252.

Stowell, M. H., Marks, B., Wigge, P., and McMahon, H. T. (1999). Nucleotide-dependent conformational changes in dynamin: evidence for a mechanochemical molecular spring. Nat. Cell Biol. *1*, 27–32.

Sweitzer, S. M., and Hinshaw, J. E. (1998). Dynamin undergoes a GTP-dependent conformational change causing vesiculation. Cell *93*, 1021–1029.

Takei, K., Haucke, V., Slepnev, V., Farsad, K., Salazar, M., Chen, H., and De Camilli, P. (1998). Generation of coated intermediates of clathrin-mediated endocytosis on protein-free liposomes. Cell *94*, 131–141.

Vallis, Y., Wigge, P., Marks, B., Evans, P. R., and McMahon, H. T. (1999). Importance of the pleckstrin homology domain of dynamin in clathrin-mediated endocytosis. Curr. Biol. *9*, 257–260.

Wang, G., Moniri, N. H., Ozawa, K., Stamler, J. S., and Daaka, Y. (2006). Nitric oxide regulates endocytosis by S-nitrosylation of dynamin. Proc. Natl. Acad. Sci. USA *103*, 1295–1300.

Wimley, W. C., and White, S. H. (1996). Experimentally determined hydrophobicity scale for proteins at membrane interfaces. Nat. Struct. Biol. *3*, 842–848.

Yoshida, Y., *et al*. (2004). The stimulatory action of amphiphysin on dynamin function is dependent on lipid bilayer curvature. EMBO J. *23*, 3483–3491.

Zhang, P., and Hinshaw, J. E. (2001). Three-dimensional reconstruction of dynamin in the constricted state. Nat. Cell Biol. *3*, 922–926.

Zheng, J., Cahill, S. M., Lemmon, M. A., Fushman, D., Schlessinger, J., and Cowburn, D. (1996). Identification of the binding site for acidic phospholipids on the pH domain of dynamin: implications for stimulation of GTPase activity. J. Mol. Biol. *255*, 14–21.

Zimmerberg, J., and Kozlov, M. M. (2006). How proteins produce cellular membrane curvature. Nat. Rev. Mol. Cell Biol. *7*, 9–19.